Development 103, 193–209 (1988)
Printed in Great Britain © The Company of Biologists Limited 1988

Regional expression, pattern and timing of convergence and extension during gastrulation of *Xenopus laevis*

RAY KELLER[1] and MIKE DANILCHIK[2]

[1]*Department of Zoology, University of California, Berkeley, CA 94720, USA*
[2]*Department of Biology, Wesleyan University, Middletown, Connecticut 06457, USA*

Summary

We show with time-lapse micrography that narrowing in the circumblastoporal dimension (convergence) and lengthening in the animal–vegetal dimension (extension) of the involuting marginal zone (IMZ) and the noninvoluting marginal zone (NIMZ) are the major tissue movements driving blastopore closure and involution of the IMZ during gastrulation in the South African clawed frog, *Xenopus laevis*. Analysis of blastopore closure shows that the degree of convergence is uniform from dorsal to ventral sides, whereas the degree of extension is greater on the dorsal side of the gastrula. Explants of the gastrula show simultaneous convergence and extension in the dorsal IMZ and NIMZ. In both regions, convergence and extension are most pronounced at their common boundary, and decrease in both animal and vegetal directions. Convergent extension is autonomous to the IMZ and begins at stage 10·5, after the IMZ has involuted. In contrast, expression of convergent extension in the NIMZ appears to be dependent on basal contact with chordamesoderm or with itself. The degree of extension decreases progressively in lateral and ventral sectors. Isolated ventral sectors show convergence without a corresponding degree of extension, perhaps reflecting the transient convergence and thickening that occurs in this region of the intact embryo. We present a detailed mechanism of how these processes are integrated with others to produce gastrulation. The significance of the regional expression of convergence and extension in *Xenopus* is discussed and compared to gastrulation in other amphibians.

Key words: convergence, extension, morphogenesis, gastrulation, *Xenopus*.

Introduction

Amphibian gastrulation is composed of region-specific morphogenetic processes that are coordinated in the intact embryo but occur autonomously and independently of one another in explants of the early gastrula (see Spemann, 1938; Schechtman, 1942; Gerhart & Keller, 1986). These morphogenetic processes are: (1) narrowing (**convergence**) and lengthening (**extension**) of the marginal zone; (2) **involution** of the marginal zone (Vogt, 1922, 1929; Schechtman, 1942); (3) spreading (**epiboly**) of the animal cap (Vogt, 1929; Spemann, 1938); (4) **invagination** of the bottle cells and their subsequent **migration** into the interior of the the gastrula (Holtfreter, 1943*a*,*b*) and (5) **migration** of the involuted mesodermal cells on the inner surface of the blastocoel roof (Holtfreter, 1944; Nakatsuji, 1974, 1975; Keller & Schoenwolf, 1977; Kubota & Durston, 1978; Nakatsuji *et al.* 1982).

Although the convergence and extension movements of the marginal zone (MZ) have been ignored in the modern literature, there is much evidence for their function in amphibian gastrulation (Vogt, 1922, 1929; chapter V, Spemann, 1938; Schechtman, 1942; Ikushima & Maruyama, 1971; reviewed in Keller, 1986), particularly in gastrulation of *Xenopus* (Keller *et al.* 1985*a*,*b*). Fate maps indicate that the MZ shows greater change in shape than any other during gastrulation (Keller, 1975, 1976) and several experimental manipulations of this region result in blockage of its involution and failure to close the blastopore (Schechtman, 1942; Keller, 1981, 1984). In contrast, these processes are not affected by removal of the bottle cells (Keller, 1981), although their formation

may aid the involution of the converging and extending MZ (Hardin & Keller, 1988). Likewise, epiboly of the animal cap (AC) and migration of involuted mesoderm over the roof of the blastocoel can be prevented by removing the entire AC, but this action does not interfere with involution of the MZ, closure of the blastopore or formation of the dorsal, axial structures in postgastrula stages (Keller *et al.* 1985*a*,*b*; also see Holtfreter, 1933).

In previous publications (Keller *et al.* 1985*a*,*b*), we presented preliminary evidence for the function and cellular mechanism of convergence and extension, which suggested that (1) the dorsal involuting marginal zone (IMZ) and noninvoluting marginal zone (NIMZ) show autonomous convergence and extension; (2) these movements begin at the midgastrula stage; (3) they are driven by active intercalation of deep cells between one another to form a longer, narrower array; (4) involution of the IMZ and closure of the blastopore is independent of mesodermal cell migration on the blastocoel roof and of epiboly of the AC.

Here we demonstrate regional differences in the capacity to exercise autonomous convergence and extension, and we document the special features of the pattern, the timing and the geometry of these movements that contribute to their function in gastrulation of *Xenopus*. Subsequent papers will examine the pattern of the cell intercalation that drives convergence and extension and also the cell motility underlying active intercalation of deep cells.

Materials and methods

Preparation of embryos and microsurgery

Xenopus laevis embryos were obtained as described previously (Keller, 1975), dejellied with cysteine hydrochloride (see Keller, 1981), and held at 15–25°C in modified Niu-Twitty solution (MNT) (phosphate and carbonate buffers replaced with 5 mM-Hepes). Vitelline envelopes were removed with sharpened watchmaker's forceps and explants were cut from embryos on a base of clay (Plasticine) or 2% agarose in an operating dish of 100% MNT, using eyebrow hairs mounted in disposable pipettes with paraffin. Halves of explants were held together by glass bridges supported at both ends by peaks of clay. After healing for 15–20 min, explants were moved to dishes with agarose-coated bottoms (2% agarose in 100% MNT) and photographed at intervals on 35 mm film. Staging was according to Nieuwkoop & Faber (1967). Stages of explants were determined from companion, control embryos kept in the same dish. 484 explants were done and analysed.

Time-lapse cinemicrography and videomicrography

Time-lapse records were made directly on 16 mm Kodak Plus X Reversal film, using a Bolex or Arriflex time-lapse camera, or on videotape with a Panasonic videocamera and time-lapse recorder. A compound microscope with bright field optics and a stereomicroscope were used with low-angle epi-illumination from a fibre optic, quartz lamp or a heat-filtered tungsten lamp. Simultaneous recordings of the surface and edge views of explants were made by using a horizontal compound microscope and vertical stereoscope together. For analysis, the film image from the vertical microscope was projected to match the size of the video image from the horizontal compound microscope.

Fixation, histology and scanning electron microscopy (SEM)

For histology, embryos were fixed in Smith's fixative, dehydrated, cleared in Histosol, embedded in Paraplast, sectioned at 10 μm and stained with haematoxylin and eosin. For SEM, embryos were fixed in 2% glutaraldehyde in 0·1 M-sodium cacodylate buffer (pH 7·4), washed in this buffer, fractured with steel knives (see Keller & Schoenwolf, 1977) and prepared for SEM on an ISI microscope by standard methods. Micrographs were made at 10 kV on Ilford sheet film.

Morphometrics, terminology and orientation

Change in the shape of explants and individual cells were quantified with a morphometrics program on a Numonics digitizer and Apple computer. For orientation, the gastrula is viewed as having an animal–vegetal (A–V) dimension, defined by meridian lines passing from the animal pole to the vegetal pole, and a circumferential dimension, defined by latitude lines perpendicular to the meridians and parallel to the margin of the blastopore. **Extension** is the lengthening of tissue in the A–V direction, measured by dividing the original A–V distance between cells into the distance separating them at some later time. **Convergence** is the narrowing of tissue along latitude lines, measured by dividing the original circumferential distance between cells into the distance separating them at some later time. We identify two marginal zones (Keller *et al.* 1985*a*,*b*). The **involuting marginal zone (IMZ)** lies immediately animal to the site of blastopore formation in the early gastrula. It consists of prospective mesoderm in the deep region and prospective endoderm in the superficial layer, both of which involute during gastrulation to form the mesodermal mantle and roof of the archenteron, respectively (Keller, 1975, 1976). The **noninvoluting marginal zone (NIMZ)** lies animal to the IMZ, and it converges and extends into the space vacated by the IMZ as the IMZ involutes. Thus, it consists of prospective ectoderm and it forms the margin of the blastopore at the end of gastrulation. The common boundary of the IMZ and NIMZ is called the **limit of involution (LI)**. Animal to the NIMZ is the **animal cap (AC)**. In traditional terminology, the NIMZ would occupy the vegetal end of the AC, but we distinguish the NIMZ from the AC because it expresses different morphogenetic movements during gastrulation (Keller *et al.* 1985*a*,*b*).

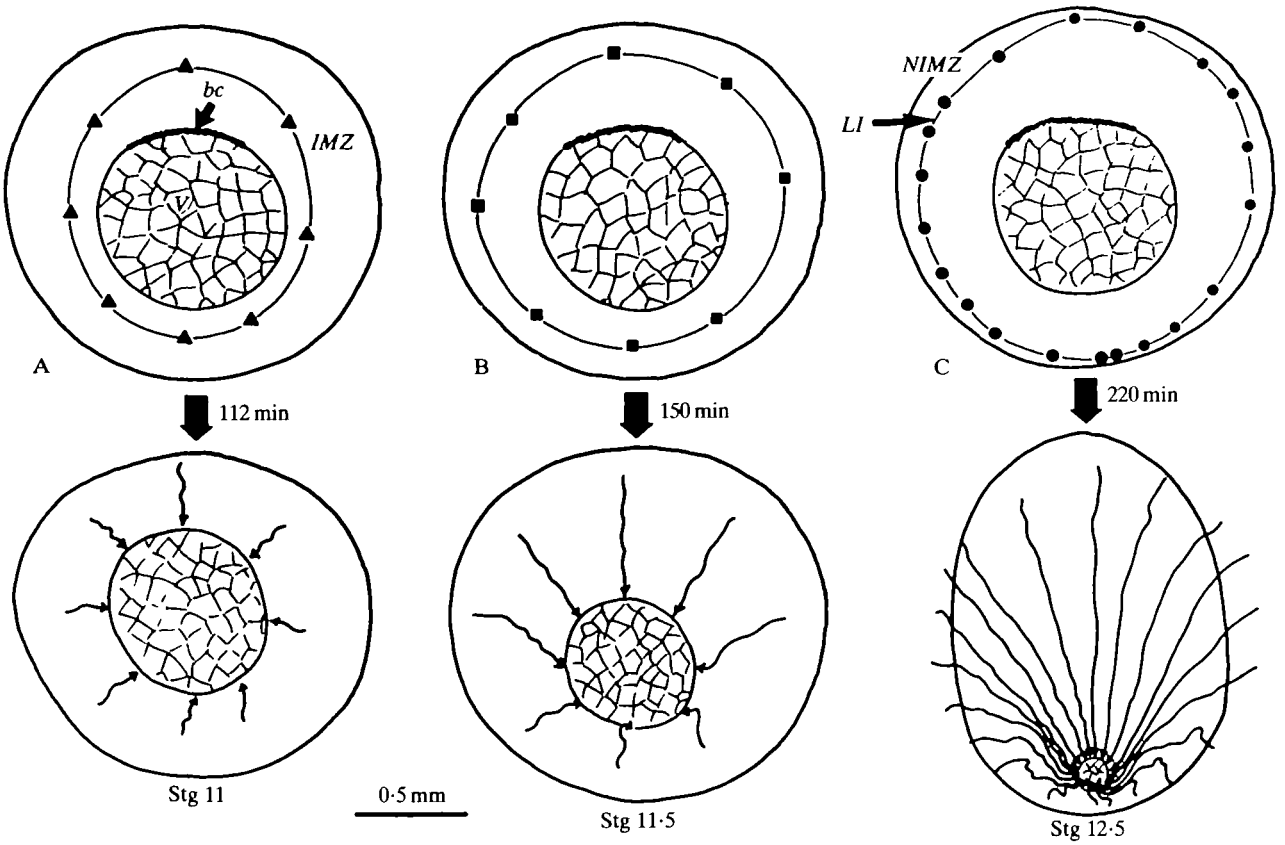

Fig. 1. The movements of cells in the involuting marginal zone (IMZ) are traced to their point of involution by time-lapse cinemicrography of the vegetal views of the gastrula. All three illustrations in the top row represent a vegetal view of the same early gastrula at stage 10+, 43 min after formation of the bottle cells (*bc*) was initiated. The symbols (triangles, squares, solid circles) indicate three roughly concentric tiers of cells located progressively higher in the IMZ. (A) Movements of cells located low in the marginal zone (triangles) are traced in route to their involution at stage 11, 112 min later. (B) Movements of the next tier of cells (squares) are traced to their point of involution at stage 11·5, 150 min later. (C) Movements of cells located at the limit of involution (LI, filled circles), where the IMZ bounds the noninvoluting marginal zone (NIMZ), are traced to their point of involution 220 min later at stage 12·5. These convergence and extension movements are quantified in Table 1.

Results

The IMZ converges and extends during its involution and during blastopore closure

Time-lapse recordings of the vegetal aspect of the gastrulating embryo show the convergence of the IMZ during its involution and closing of the blastopore (Fig. 1). Movements of three tiers of IMZ cells, located at successively higher levels in the IMZ of the early gastrula (stage 10+), were traced to their point of involution (Fig. 1; Table 1). Five main points emerge from these data. First, cells located in tiers higher in the IMZ, and thus involuting later, undergo more convergence than those located lower and involuting earlier (Fig. 1; Table 1). Thus, considering only cell movements up to the point of involution, there is a progressive increase in convergence of the IMZ, from a minimum at its vegetal end to a maximum at its boundary with the NIMZ (the LI). A tenfold convergence of cells at the LI (Table 1) represents the loss of about 4200 μm (18 min^{-1}) of circumference and results in closure of the blastopore by the end of gastrulation. Second, the absolute amount of convergence is nearly uniform in all sectors of the circumblastoporal region. Third, extension, as reflected by the rate and the total amount of movement of IMZ cells toward the blastoporal lip (BPL), is greatest in the dorsal sector and decreases laterally and ventrally. In the dorsal sector of the gastrula, the rate of advance of IMZ cells toward the BPL increases with increasing distance from the blastopore and with involution at later times (Table 1). Thus those cells nearest the LI move farther and faster than their counterparts nearer the vegetal end of the IMZ. Fourth, the rate of advance of the BPL is always less than that of the IMZ cells, and thus the IMZ overtakes the BPL and involution occurs. The disparity in rate, taken over the whole of gastrulation for the cells located at the LI, is by a factor of about 1·5

Table 1. *Convergence and extension*

Stage at which cells involuted	Convergence*			Extension†			
	Whole	Dorsal	Ventral	Dorsal	Dorso-lateral	Ventro-lateral	Ventral
11	0·66	0·64	0·69	317	238	214	206
	(11)			(2·8)	(2·1)	(1·9)	(1·8)
				[−0·3]	[−0·1]	[0·8]	[0·9]
11.5	0·44	0·46	0·42	523	507	262	270
	(15)			(3·7)	(3·4)	(1·7)	(1·8)
				[1·4]	[1·1]	[0·4]	[0·2]
12·5	0·10	0·10	0·10	1266	1079	711	289
	(18)			(5·6)	(4·8)	(3·1)	(1·3)
				[3·8]	[2·8]	[2·3]	–

* Convergence is defined as the circumferential distance between cells at the end of the period in question divided by the original distance between them. See Materials and methods for details. The rate of loss of circumference is indicated in $\mu m\ min^{-1}$ in parentheses.

† Extension is defined as the elongation of the circumblastoporal region in the animal–vegetal direction The values given here are for displacements of cells in the vegetal direction, a parameter which reflects extension of both IMZ and NIMZ.

Rate of extension ($\mu m\ min^{-1}$) is indicated in round parentheses for cells and in square parentheses for BPL.

(Table 1). Because of the greater extension there, cells in the dorsal sector move much farther before their involution than those located laterally and ventrally. This disparity results in the displacement and closure of the blastopore farther ventrally than would have occurred if extension were uniform. Fifth, between stages 10+ and 10·5, the rate of advance of the IMZ cells and the blastoporal lip is nearly the same in all sectors, whereas after stage 10·5, movement of both in dorsal and dorsolateral sectors is relatively faster. The initial movements of the IMZ prior to stage 10·5 are due, in part, to bottle cell formation (Hardin & Keller, 1988).

The NIMZ converges and extends to close the blastopore during normal gastrulation

As the dorsal IMZ converges and involutes, the dorsal NIMZ converges and extends behind it. Local rates of extension were determined by recording the changing positions of individual cells in five tiers between stages 11 and 12 (Fig. 2). It is apparent that cells with initial positions nearer the BPL move greater distances and faster than those farther away. The degree of convergence and extension of the NIMZ, measured locally, increases progressively with proximity to the LI (from tier 3 through tier 1, Fig. 3). Tier 3, located about three quarters of a millimeter above the blastoporal lip at stage 11, marks the transition from the uniformly and slowly spreading behaviour of the AC toward the rapid spreading, convergence and extension of the dorsal NIMZ (see Fig. 5, Keller, 1978). Extension of the

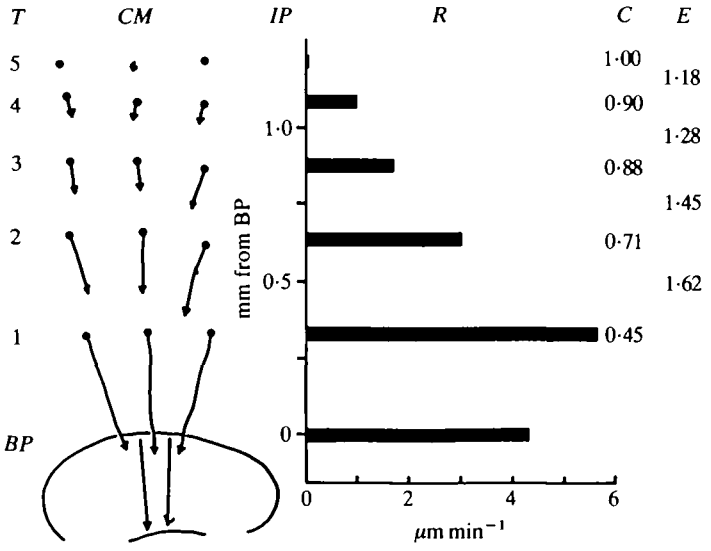

Fig. 2. The movements of individual cells in the dorsal NIMZ are traced over a period of 72 min, from stage 11 to stage 12, by time-lapse cinemicrography. The cell movements (*CM*) are indicated by arrows. The cells are arrayed in five tiers (*T*), numbered in order of increasing distance from the blastoporal lip (*BP*). The mean rates of movement of each of these tiers of cells (*R*) toward the BPL are plotted against their initial positions (*IP* in mm) with respect to the BPL. The rate of movement of the BPL itself (IP = 0) is also shown. The degree of convergence (*C*) of the points in each tier and the degree of extension (*E*) for each interval between tiers is indicated at the left. Since extension was underway at the beginning, mean rates are calculated by dividing total distance moved by time elapsed.

NIMZ decreases progressively in lateral and ventral sectors, as it does in the IMZ (Fig. 1), a fact reflected in the decreased movement of the LI vegetally in these sectors (Fig. 1C). Convergence and extension of the dorsal NIMZ continues unabated and without abrupt change in rate, into the neurula where these movements contribute to the narrowing and lengthening of the posterior neural plate. As in the gastrula stage, convergence and extension increase progressively nearer the blastopore.

Dorsal explants of the early gastrula show two regions of autonomous, graded convergence and extension

'Sandwich' explants were made by excising a large dorsal sector of two early gastrulae as shown (Fig. 3A,B) and sandwiching their deep surfaces together (Fig. 3C) (Ikushima & Maruyama, 1971), after which they were cultured on agarose-coated dishes and observed by time-lapse recording. 157 explants were made; 45 were filmed or videotaped,

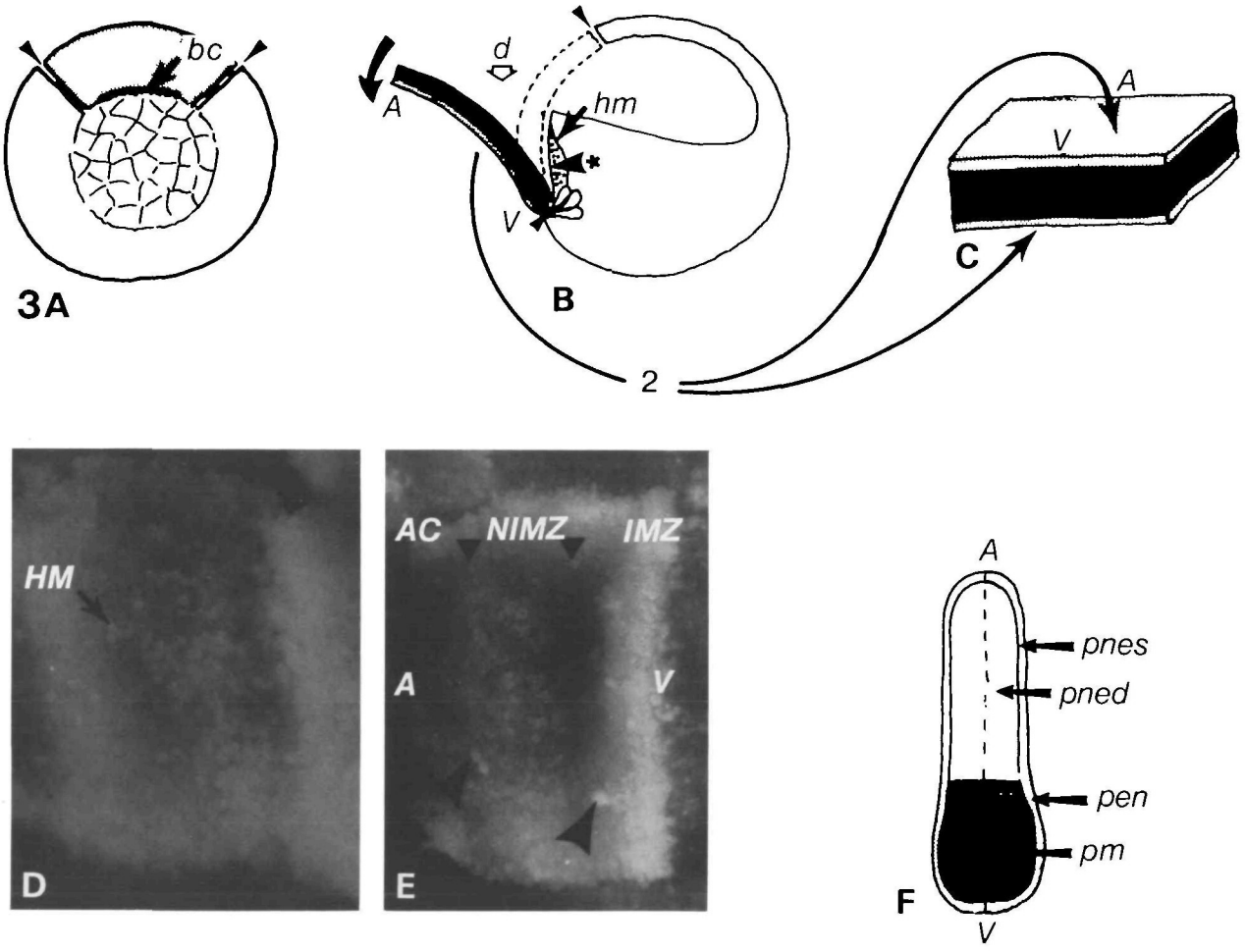

Fig. 3. Steps in making a 'sandwich' explant of the dorsal sector of the gastrula are shown. Cuts, indicated by tapered pointers, are made first along dorsolateral meridians of the early gastrula (A), and the flap of tissue is then cut at the animal pole and pulled vegetally (curved arrow in B). The inner surface is teased away from the deeper, involuted region (at the asterisk), which is the prospective head mesoderm (*hm*). The explant is then cut off vegetally at the level of the bottle cells (*bc*). The inner surfaces of two such rectangles of tissue are apposed and pressed together (C) with a coverslip bridge until healing occurs (15 min). The animal (*A*) and vegetal (*V*) ends of each are kept in register. If the explant is not cleanly teased away from the involuted material, some of the larger, yolky head mesodermal cells (*HM*) may stick to its inner surface (*d*). These must be cleaned off with a hair loop until few (pointers in E) or none remain. The approximate positions of the involuting marginal zone (*IMZ*), noninvoluting marginal zone (*NIMZ*) and the animal cap (*AC*) are shown in E. The prospective fates of the superficial and deep layers of the explant, extrapolated from the fate map of the normal gastrula (Keller, 1975, 1976) are approximated in a schematic sagittal section of an explant (F): *pnes*, prospective neural ectoderm, superficial; *pned*, prospective neural ectoderm, deep; *pen*, prospective endoderm; *pm*, prospective mesoderm. Magnification of D,E, ×42. Bar, 0·5 mm.

two in edge and surface view, simultaneously. These explants consistently showed characteristic regional differences in morphogenetic movements and tissue differentiation (see Fig. 4) which were mapped back on to the original explant, providing, retrospectively, the basis for dividing it into IMZ, NIMZ, and AC regions. The IMZ–NIMZ boundary (LI) is about 0·25–0·3 mm above the blastopore and is marked by a transition from the larger, yellow IMZ cells to smaller, greyer NIMZ cells, and by the greater thickness of the former region (Fig. 3E). The NIMZ–AC border has no visual indicators at stage 10+. This boundary is operationally defined in dorsal explants as the zone of transition from uniform slow epiboly of the AC to rapid spreading and convergence and extension of the NIMZ, mentioned above. It can be mapped back, in stage 10+ explants, to about 0·5–0·6 mm above the blastopore (Fig. 3E). After healing, the explant consists of a continuous epithelial sheet and a deep region consisting of several layers of nonepithelial cells (Fig. 3F). For reference, prospective fates are approximated (Fig. 3F) from fate maps (Keller, 1975, 1976).

The dorsal sandwich autonomously thins, converges and extends, increasing its animal–vegetal dimension by some fourfold, without use of an external substratum. Explants made at stage 10 or 10+ do not begin convergence and extension until stage 10·5. The vegetal end of the IMZ initially thickens somewhat and then thins, converges and extends (arrows at 0 and 0·25 h, Fig. 4A). The region of convergence proceeds toward the LI as extension continues. Meanwhile, similar convergence and extension begin in the NIMZ ($t = 0{\cdot}25$–$0{\cdot}5$ h, Fig. 4A). Convergence and extension activities are considerable by the end of gastrulation ($t = 1{\cdot}5$ h, Fig. 4A) and continue through the early neurula stage ($t = 2{\cdot}5$, Fig. 4A) and beyond. In the late neurula and early tailbud stages ($t = 3{\cdot}5$–$6{\cdot}5$ h, Fig. 4A), the AC end of the explant begins to round up and swell to form a fluid-filled vesicle.

The NIMZ extends faster than the IMZ, by a factor of 1·7 (average from 15 time-lapse records; these data are presented as ratios rather than absolute rates because the temperature varied from 15 to 25 °C) and it shows greater translation of width and thickness into length (Fig. 4A), narrowing to less than a quarter of its original width compared to just under half for the IMZ. Both regions thicken by about 10 % at the beginning but then thin during convergence and extension to reach 40 % (NIMZ) and 50 % (IMZ) of their original thickness. As convergence and extension proceed, the NIMZ mimics the neural plate in that it becomes thinner at the midline than at each edge and forms a central groove (pointers in Fig. 4B). It develops into a mass multipolar, neurone-like cells at tailbud stages and does not stain with fluorescein-ated peanut lectin (E. Wahl, unpublished experiments), suggesting that it is, in fact, neural tissue (see Slack, 1985). As convergence and extension proceed in the IMZ, a notochord forms centrally at stage 11·5, flanked on either side by somitic mesoderm, which segments into somites from the anterior to posterior beginning in the late neurula stages (Fig. 4C; see Keller *et al.* 1985*a*,*b*).

The pattern of autonomous convergence and extension in the dorsal IMZ and NIMZ was determined by following the displacement of individual cells of dorsal explants by time-lapse recording. Maximum convergence and extension occur at the LI, and decrease progressively in the animal and vegetal directions. Tracings of cells on the midline of each region (*CM*, Fig. 5) show an increased rate of movement (*R*) for cells with initial positions (*IP*) nearer the LI in each region. Moreover, the local rate of extension (*E*) increases in intervals nearer the LI in both the IMZ and NIMZ. The greater extension in regions closer to the LI is probably due to the pattern of convergence; cells move in arcs directed medially and toward the LI (Fig. 4A).

In summary, the tissues of the dorsal sandwich explants autonomously display two regions of endogenously driven, highly patterned convergence and extension, and differentiate into recognizable larval structures characteristic of the same regions in the intact embryo.

Active convergence and extension of the IMZ occur after its involution

Sandwich explants made from early gastrulae do not begin convergence and extension until about stage 10·5, at which time they begin abruptly. Thus when convergence and extension begin, the vegetal end of the IMZ would have already involuted in the intact embryo. In 12 explants made from stage 10·5 embryos, the IMZs did not elongate as much as their counterparts made at stage 10+ and they contained only the posterior third to a half of the notochord (Fig. 6A,B). In all cases, the complementary piece of anterior notochord developed in the embryo from which the explant was taken (Fig. 6C). These facts argue that the vegetal end of the IMZ has involuted before it begins active convergence and extension at stage 10·5.

Dorsoventral patterning of convergence and extension

To resolve the pattern of circumblastoporal convergence and extension, but in a planar form, we analysed the morphogenetic movements in large explants, consisting of the entire dorsoventral aspect of the marginal zone (Fig. 7). Such explants were

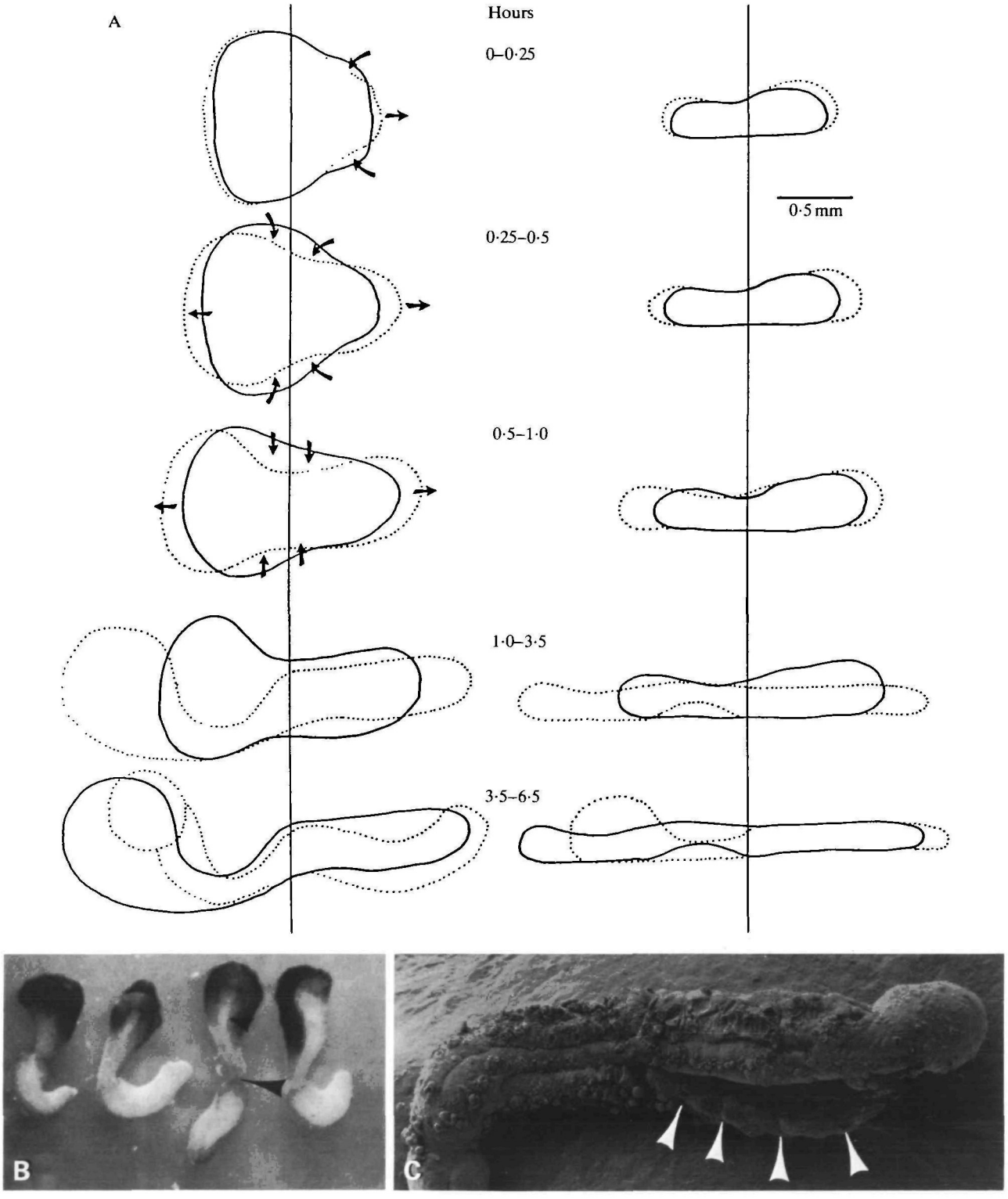

Fig. 4. Outline tracings of an explant made at stage 10·5 in surface view (left column) and lateral view (right column), were made from simultaneous filming and videotaping of these aspects of a dorsal explant (A). Elapsed time is shown in hours and the vertical lines passing through all explants show the limit of involution (LI), separating the NIMZ (left) and the IMZ (right). The shape of the explant at the beginning of each time interval is indicated by solid lines and the change in shape in the following period is indicated by dotted lines. A light micrograph (B) shows explants equivalent to those shown in the 3·5 h outlines. The large pointer indicates the junction of the IMZ and NIMZ and the small one indicates the groove in the central part of the NIMZ. An SEM of the IMZ from which the covering layer of endoderm has been removed (C) shows the central notochord flanked on either side by the somitic mesoderm, which segments (arrows), forming somites in the anterior-to-posterior direction. Magnifications: B, ×13; C, ×80.

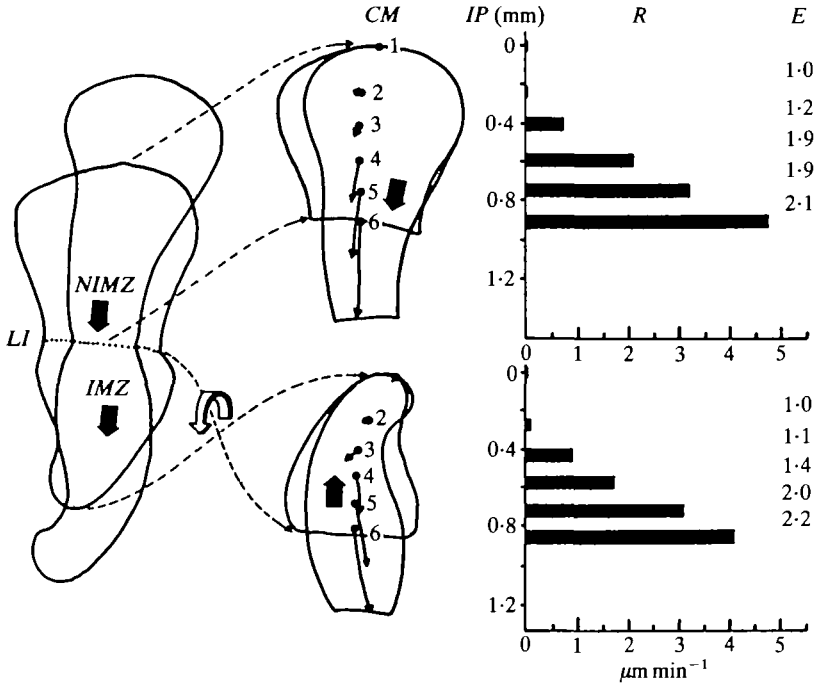

Fig. 5. The two outlines at the far left show the change in shape of a dorsal explant during a 67 min interval between stages 11 and 12. The animal–vegetal polarity of the NIMZ and IMZ are shown with large arrows and the limit of involution (*LI*) is indicated by a dotted line. In the middle diagram, cell movements (*CM*), traced by time-lapse cinemicrography, are indicated by arrows. For purposes of illustration, the IMZ and NIMZ are separated at the LI and the animal–vegetal polarity of the latter is reversed, as would have been the case after its involution in the intact gastrula. The rates of movement (*R*), in micrometers, of individual cells are plotted against their initial position (*IP*) with respect to the animalmost end of each region. The degree of local extension (*E*) in intervals between the cells shown in the NIMZ and IMZ are indicated. Since extension was underway at the beginning of the sequence, rates of movement were calculated (distance over time) for the entire period. Magnification: ×30.

allowed to develop either intact (Fig. 8) or as a dorsal-to-ventral series of small explants made from the large one by meridional cuts (Fig. 10).

37 intact dorsoventral explants were made and analysed; 8 of these were filmed or videotaped. Intact explants show convergence and extension of the dorsal sector of both the IMZ and NIMZ regions, and these two regions become 'jack-knifed' at their juncture (Fig. 8A). A detailed analysis of movements shows how this shape is generated (Fig. 8B). Convergence is first seen on the dorsal side as the dorsoventral narrowing and thickening of regions 1 and 2 at the vegetal end of the dorsal IMZ (0–1 h). Convergence proceeds as the animal region of sector 1 turns counterclockwise in the vegetal direction and its middle region begins extension (3·5 h, arrows). Complementary, clockwise movements, reflecting convergence and extension, occur in regions 5 and 9 of the NIMZ (1–3·5 h). The result is an indentation of the dorsal side of the explant at the boundary of the IMZ and NIMZ. Progressively more ventral sectors, on either side of the LI (sectors no. 6, 7 10, and 11) converge, extend and are rotated, clockwise in the NIMZ and counterclockwise in the IMZ (arrows, 3–4·5 h). The process continues (not shown) until the explant becomes constricted at the LI and forms the jack-knife morphology (Fig. 8A). The greatest convergence and extension occur in the dorsal sectors of the IMZ and NIMZ near the LI. The animalmost, ventral sectors of the NIMZ (sectors no. 15 and no. 16) and the vegetalmost ventral sectors of the IMZ (sectors no. 3 and no. 4) show the least distortion of any kind. Lateral and ventral regions of both the IMZ and NIMZ converge nearly as much as their dorsal counterparts, but extension decreases in progressively more ventral regions, particularly in the IMZ, where convergence seems to be coupled with a transient thickening, from which cells spread along the ventral boundary of the somitic mesoderm.

Tissue differentiation in these explants follows that expected if the fate map of the early gastrula (Keller, 1975, 1976) were superimposed on the explant and mapped according to the distortion pattern shown in Fig. 8B, with a single notochord located dorsally (Fig. 9B), a single mass of somitic mesoderm lateral to the notochord (Fig. 9B), which segments normally from anterior to posterior (Fig. 9C), and unsegmented lateroventral mesoderm distributed along the

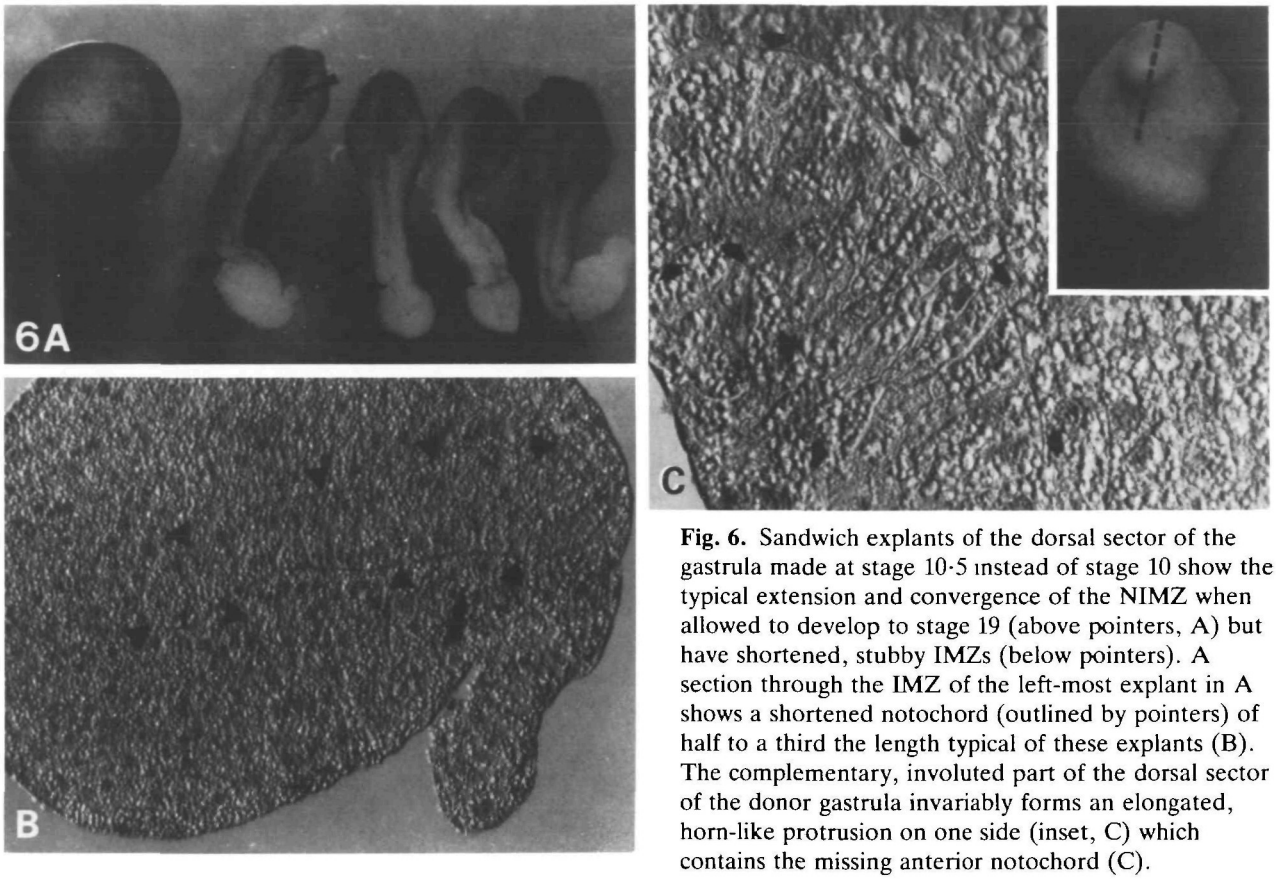

Fig. 6. Sandwich explants of the dorsal sector of the gastrula made at stage 10·5 instead of stage 10 show the typical extension and convergence of the NIMZ when allowed to develop to stage 19 (above pointers, A) but have shortened, stubby IMZs (below pointers). A section through the IMZ of the left-most explant in A shows a shortened notochord (outlined by pointers) of half to a third the length typical of these explants (B). The complementary, involuted part of the dorsal sector of the donor gastrula invariably forms an elongated, horn-like protrusion on one side (inset, C) which contains the missing anterior notochord (C).

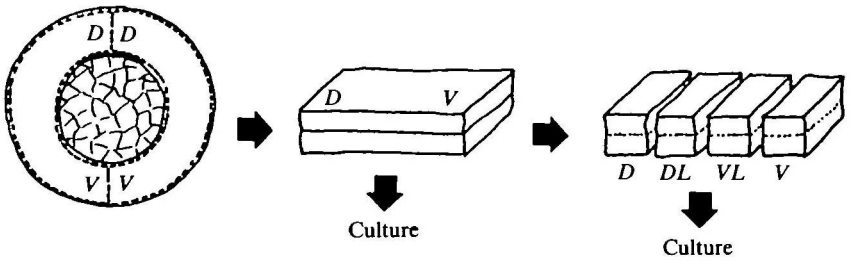

Fig. 7. The preparation of explants of the entire dorsal (D) to ventral (*V*) extent of the circumblastoporal region of the gastrula is shown diagramatically. Such an explant was left intact or divided into dorsal (*D*), dorsolateral (*DL*), ventrolateral (*VL*), and ventral (*V*) pieces.

outer, lateral borders of the somites in an unbroken sheet (Fig. 9D). A tangled mass of multipolar, neurone-like cells bearing long, intertwined protrusions form in the dorsal NIMZ (Fig. 9E) and in the AC vesicle (Fig. 9F).

57 dorsoventral explants were made and 8 were cut into halves, 22 into thirds, 24 into fourths, and 3 into fifths, as diagramed in Fig. 7. Of the 176 explants thus generated, 57 were recorded in time-lapse mode and analysed in detail. In addition, 53 lateral quarters and 48 ventral quarters were analysed. The degree of convergence and extension shows the dorsal-to-ventral pattern seen in the intact gastrula and in whole dorsoventral explants. Convergence and extension occur in dorsal thirds, fourths and fifths but are progressively less in the fourths and fifths, even though the dorsalmost region of each explant represents the same tissue region and undergoes identical and maximal convergence and extension *in situ* (Fig. 10A–C). The lateral thirds, and dorsolateral fourths and fifths invariably show some convergence and extension, and develop into notochord and somites (Fig. 10E). The ventral thirds and ventrolateral fourths and fifths show less extension, become rotund (Fig. 10B–D), and usually develop mesenchyme and blood. Ventral sectors did not show more dorsal behaviour when isolated at stage 10·5 than when isolated at stage 10. The lateral thirds and occasionally ventrolateral fourths show some convergence and extension to produce a tapered vegetal end (Fig. 10A,B). A given ventrolateral region is more likely to show convergence and extension as part of a larger explant than as part of a smaller one. The ventral thirds and sometimes the ventrolateral and ventral fourths and fifths show a cryptic convergence, without a corresponding degree of extension, associated with involution of the IMZ. The deep mesoderm of the IMZ involutes to form a thickened ring of

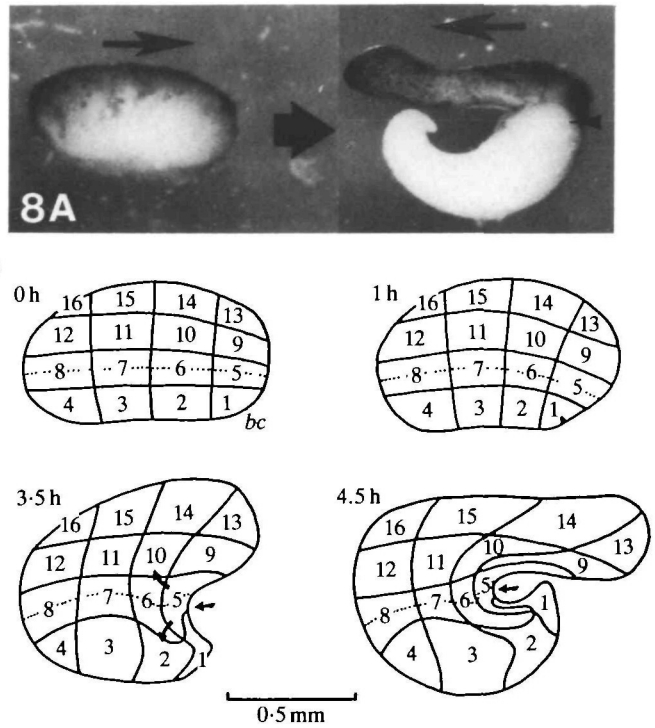

Fig. 8. The initial and final states (stage 18) in the development of a dorsoventral explant is shown (A). The arrows point dorsally in each micrograph. The pattern of distortion of a dorsoventral explant (B), determined by time-lapse cinemicrography, is represented by the distortion of a grid superimposed on the explant shortly after its formation (0 h) at stage 10+ and followed through the middle (1 h) and late gastrula stages (3·5 and 4·5). The LI is indicated with a dotted line. The site of the blastopore is marked by a few remaining bottle cell apices with dark pigment (*bc*).

mesoderm inside the blastoporal lip and the endoderm involutes to form a short archenteron (Fig. 10F). As this occurs, the NIMZ of the explant converges around the blastopore and the animal end of the involuted mesoderm thins and spreads over the entire inner surface of the NIMZ-AC (arrows, Fig. 10F). A dimple in the vegetal end of the explant marks the blastopore (pointers in Fig. 10A,C).

The total convergence and extension of isolated dorsoventral sectors is less than that of whole dorsoventral explants and thus the sum of the LIs of the component fragments is greater than the LI of the whole explant (compare the sum of LIs at the pointers in Fig. 10B with the LI of the intact explant in Fig. 8A, which is at the same scale).

The deep nonepithelial cells drive convergence and extension

Eight sandwich explants were made from embryos in which the native superficial epithelium of the dorsal sector was either removed and replaced (four cases) or was replaced with the epithelium from the AC (four cases), a region which ordinarily does not show convergence and extension. In all cases, the IMZ and NIMZ converged and extended (Fig. 11A,B), though not as much as normal explants. Thus both epithelia appear to support or at least allow some convergence and extension. However, an epithelium of some sort appears to be necessary. The deep cell population alone, without any epithelium, failed to converge and extend, either in MNT or in Danilchik's solution (see Keller *et al.* 1985*a*,*b*). Conversely, sandwiches of epithelial sheets from all sectors of the gastrula did not show convergence or extension but formed wrinkled balls. Convergence and extension of the deep AC or the ventral marginal zone could not be induced by transplantation of the epithelium from the dorsal NIMZ or IMZ (data not shown).

Discussion

Convergence and extension are autonomous, region-specific properties of the IMZ

Our analysis of intact gastrulae and tissue explants reveals a highly organized pattern of convergence and extension (Fig. 12). Both convergence (Fig. 12A) and extension (Fig. 12B) are maximum near the LI in the prospective posterior sectors of both the IMZ and NIMZ. In any dorsoventral region, extension decreases from a maximum at the LI (prospective posterior region) toward a minimum in the prospective anterior regions, i.e. animally in the NIMZ and vegetally in the IMZ (Fig. 12A,B). In the prospective dorsal posterior sectors of both the NIMZ and IMZ, convergence and extension are coupled (Fig. 12C), and tissue volume is apparently conserved. For this reason, the two processes can be referred to as **convergent extension** (see Keller *et al.* 1985*a*,*b*). Convergent extension occurs in sandwich explants of the gastrula, indicating that it is a local, autonomous process, not requiring substrata or source of mechanical force. Although an epithelial covering is required, the deep mesodermal cells generate the force for convergent extension. In the ventral regions, very little extension accompanies convergence and thus the two processes are uncoupled (Fig. 12A–C). Such convergence without a corresponding degree of extension raises the question of where the tissue concentrated by convergence goes.

The following hypothesis about morphogenetic behaviour of the prospective mesoderm accounts for most of the facts from this study and others. The mesoderm undergoes a sequence of behaviours beginning in the prospective anterior (vegetal IMZ) and passing posteriorly (animal IMZ). First, there is an initial and transient phase of **convergence and thickening** in which the tissue thickens at the expense of

width. This accounts for the transient thickening of the IMZ preceding its extension. Second, a phase of **thinning and extension** occurs as the mesoderm thins and spreads rapidly due to **radial intercalation** of several layers of cells to form fewer layers (Keller, 1980). This behaviour accounts for the initial thinning and extension of the IMZ. In the third phase, the mesoderm undergoes one of two alternate behaviours, depending on the type of mesoderm. The prospective dorsal, posterior (notochordal and somitic) mesoderm undergoes **convergence and extension**, brought about by **mediolateral intercalation** of cells (see Keller *et al.* 1985*a*,*b*). In contrast, the prospective dorsal anterior (head) meosderm, the

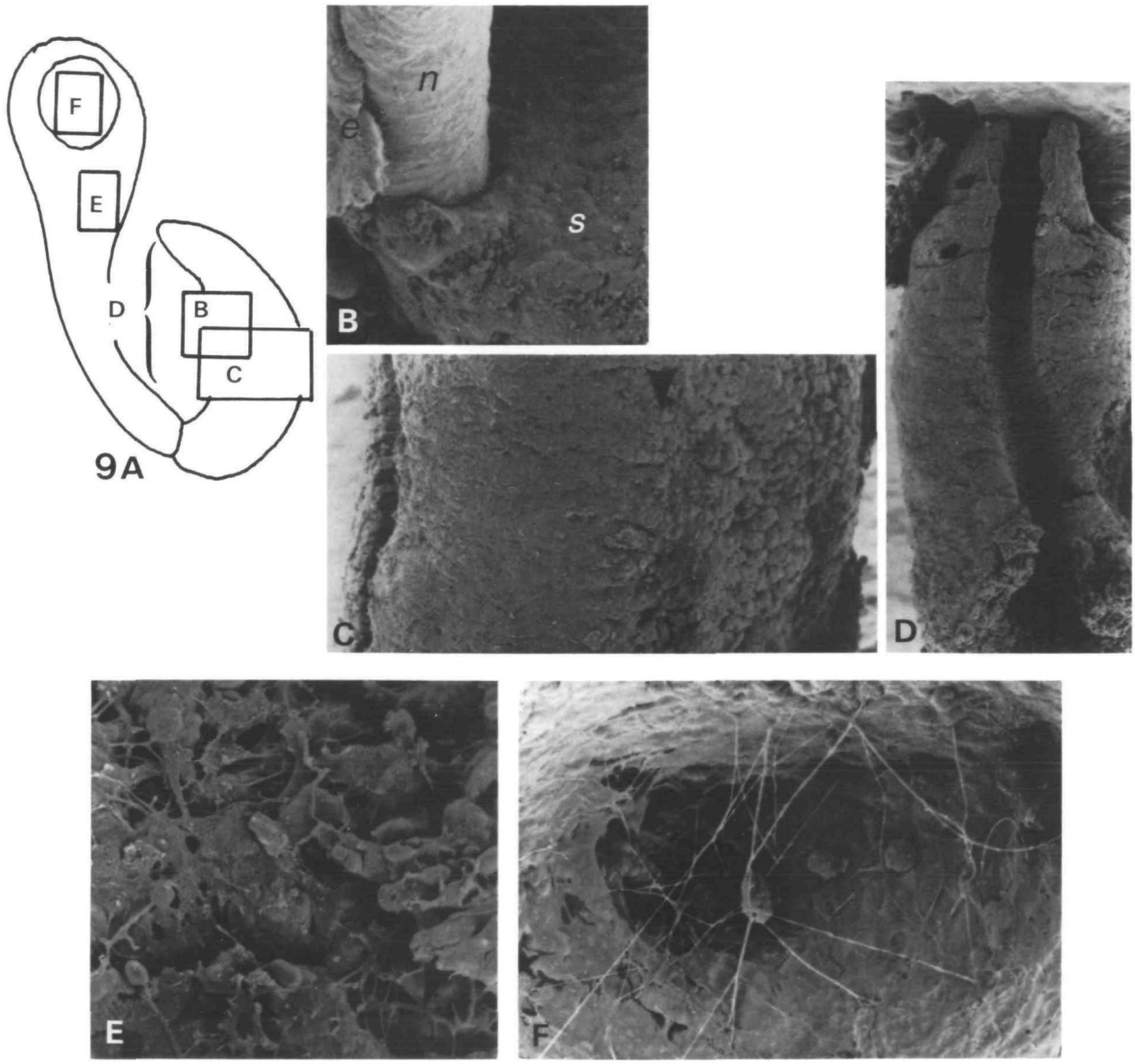

Fig. 9. A outline drawing of a dorsoventral explant at the early tailbud stage is shown (A) for orientation of SEMs taken in various regions (B–F). The dorsal side of the IMZ contains a notochord (*n*) abutting on the superficial endoderm (*e*), which forms the epithelium covering the IMZ of the explant (B). Ventral to the notochord is a single mass somitic mesoderm (*s*) that encircles the notochord, except where it bounds the endoderm dorsally (B). Somitic mesoderm segments from anterior to posterior (arrows at right in C) as in normal development. Farther ventrally, the parallel arrays of elongated somitic cells (*s*) give way to rotund, lateral mesodermal cells, which do not show elongation, orientation, or segmentation (to the right of the pointer, D). The shaft of the elongated NIMZ consists of multipolar cells bearing long protrusions which are entwined and tangled, making fracture difficult (E). The AC forms fluid-filled cavities and these often contain rotund cells with multiple protrusions several hundred micrometres long (F). Magnifications are: B, ×423; C, ×182; D, ×344; E, ×1240; F, ×850.

lateral mesoderm and the ventral mesoderm undergoes **spreading** by the **migration** of individual cells out of the IMZ and across the blastocoel roof. These behaviours follow one another, beginning at the vegetal (prospective anterior) end of the IMZ and passing to the animal (prospective posterior) end, and occurring first dorsally and then ventrally. Thus, at the end of gastrulation, convergence and extension is well underway in the dorsal posterior sector, whereas convergence and thickening is just beginning in the ventral posterior sector and accounts for the presence of the thickened annulus of mesoderm just inside the ventral BPL of the late gastrula (Keller, 1976). The fact that the occurrence of convergence and extension dorsally is balanced by simultaneous convergence and thickening ventrally explains the mechanical integrity of the ventral sector noted in this work and by Schechtman (1942), and it explains the fact that convergence is coupled with invagination (migration) in ventral sectors and with extension in dorsal sectors

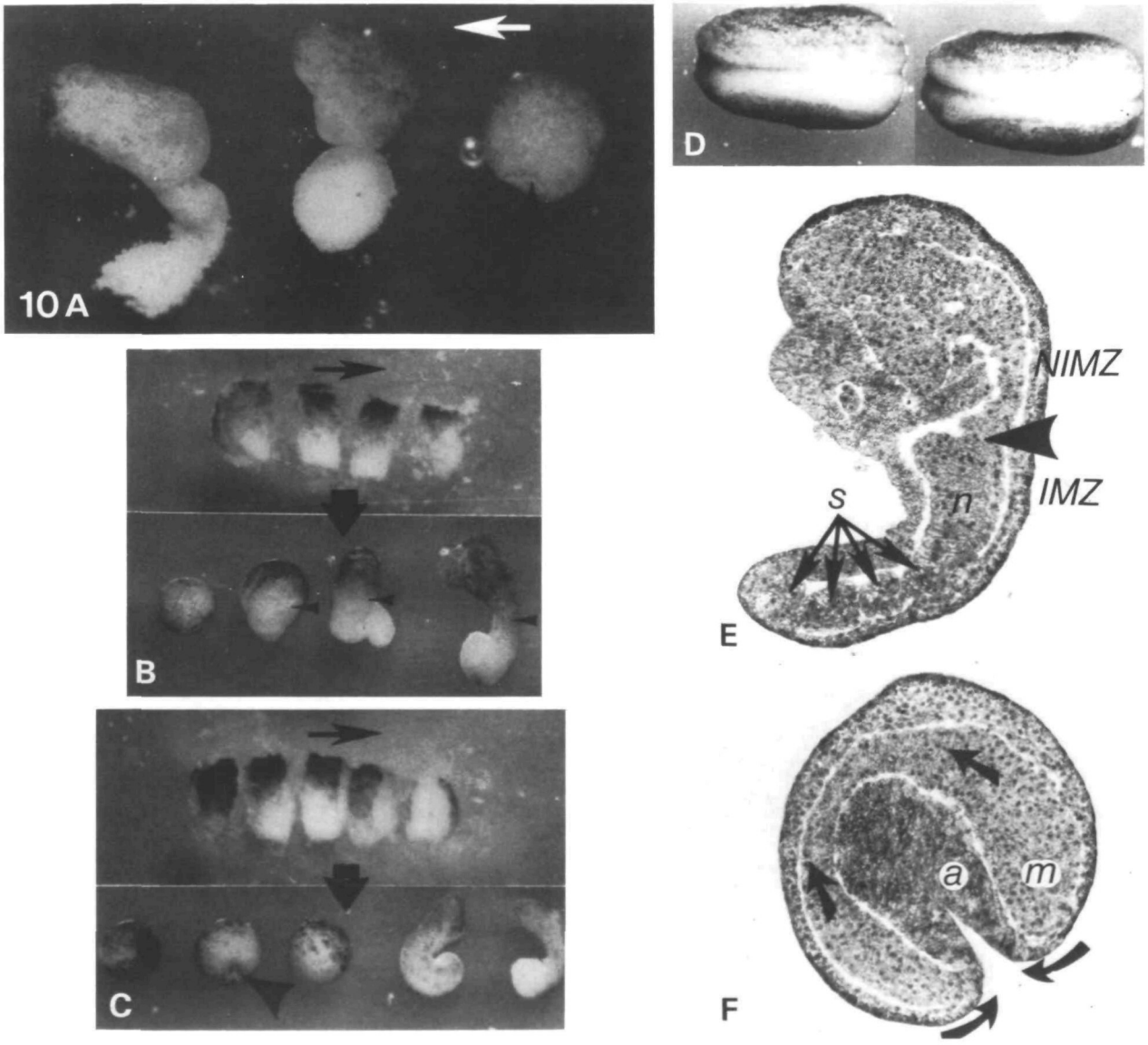

Fig. 10. The development of explants divided into thirds (A), fourths (B), or fifths (C) to the equivalent of stage 18 is shown. The arrows at the top of each photo point toward the dorsal side of the explant or array of explants (B,C). The small pointers indicate the LI in each explant or fragment thereof (B). Dorsal views of control neurulae, anterior ends to the left, are shown (D). A section through a lateral third explant (E), allowed to develop to the tailbud stage, shows somites (*s*) anteriorly and notochord (*n*) posteriorly in the IMZ, and abutting on the NIMZ. A section through a ventral explant (F) shows the involuted mesoderm (*m*) and a short archenteron (*a*). The curved arrows show the convergence movements at the blastopore and the animalward migration of the leading mesoderm. Large pointers (A,C) show sites of involution in ventral explants.

(Schechtman, 1942). Subsequently, in the early neurula stage, the thickened ring of mesoderm disappears as it undergoes the second and third phases; it undergoes thinning and spreading and then is added either to the posterior somitic mesoderm by convergence and extension or to the ventral mesodermal mantle by migration (see Vogt, 1929; Keller, 1976).

Explant size and dorsoventral interactions

In a given dorsoventral sector of the IMZ, larger explants show greater convergent extension than small ones. There may be something intrinsic to the process of deep cell intercalation (see Keller & Hardin, 1987) that allows convergent extension to occur more effectively if there is a large population of cells that participates from the outset or from which participants can be recruited. The amount of convergent extension may be determined by the size of the participating cell population; at any anterior–posterior level of the IMZ, it is directly proportional to the amount of prospective dorsal, axial mesoderm (notochord and somite) occupying that level (Fig. 12A,B). Thus the fact that the prospective notochord and somite areas extend farther ventrally in their prospective posterior regions (closer to the LI) reflects their greater convergent extension in the course of gastrulation (Fig. 12E).

There is evidence of long standing that the various dorsoventral sectors of the marginal zone have differing intrinsic capacities of differentiation; on the other hand, it is well established that the dorsal marginal zone can dorsalize ventral tissues (see Spemann, 1938; Holtfreter, 1938*a*,*b*; Cooke & Weber, 1985*a*,*b*; Dale & Slack, 1987). The dorsal IMZ may affect the ventral IMZ through mechanical interactions, as argued by Schechtman (1942), entraining it to extend more than it might in isolation. Our data support this idea, at least qualitatively. However, we cannot distinguish between nonmechanical signals passing from dorsal to ventral tissues and mechanical towing of contiguous ventral tissues. If nonmechanical interaction between dorsal and ventral regions does persist well into the gastrula stage (and the evidence suggests that it does at least until the early gastrula stage; see Spemann, 1938; Slack & Forman, 1980; Dale & Slack, 1987), convergence and extension would increase its effectiveness by bringing dorsal and ventral tissues closer together.

A second, contact-dependent convergent extension occurs in the NIMZ

The dorsal NIMZ converges, thins and extends in explants as it does in the gastrula (Keller, 1975, 1976, 1978, 1980) and in the neurula (Keller, 1975, 1976), mimicking the behaviour of the central neural plate (notoplate; see Jacobson, 1981). Tangled multipolar cells resembling neurones or glial cells differentiate in the dorsal NIMZ and the region does not stain with fluoresceinated peanut lectin, a trait of *Xenopus* neural tissue (see Slack, 1985). This putative neural character of the dorsal NIMZ is less likely to result from its brief contact with involuted head mesoderm, prior to explantation at stage 10–10+ (see Akers *et al.* 1986) than from its continued association with the mesodermal IMZ at the LI (see Kintner & Melton, 1987). In any case, both routes of tissue interaction – the association of NIMZ and IMZ at their common boundary and the growing basal contact between them – are more prominent *in vivo* than in the

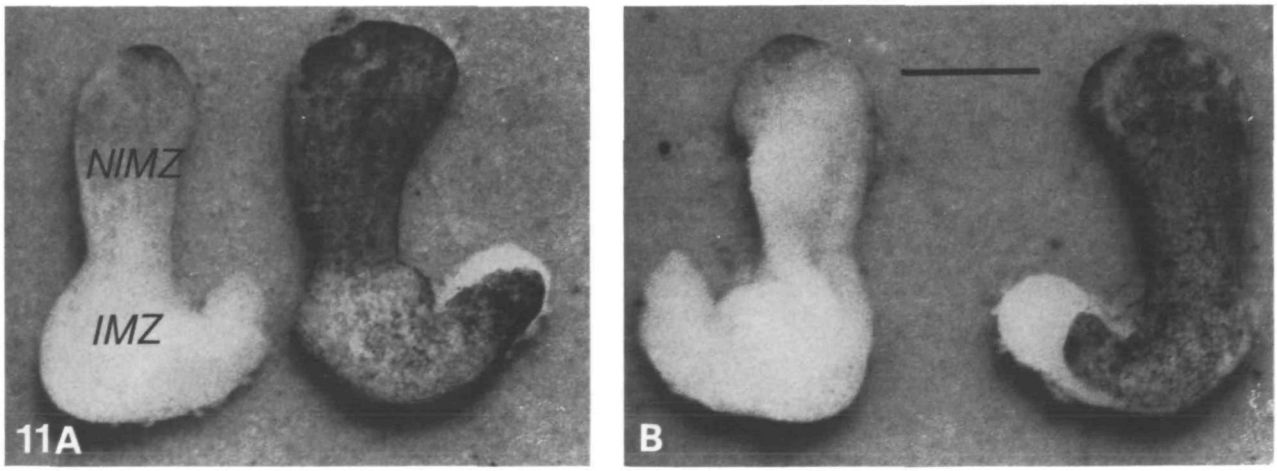

Fig. 11. Both sides of (A,B) of two dorsal explants of the early gastrula are shown after development to the late neurula stage. The left explant was made from embryos in which the superficial epithelium was removed and replaced prior to making the explant. The right explant was made from an embryo in which the superficial epithelium of the dorsal IMZ and NIMZ was replaced with the heavily pigmented epithelium from the AC. Both the IMZ and NIMZ converged and extended.

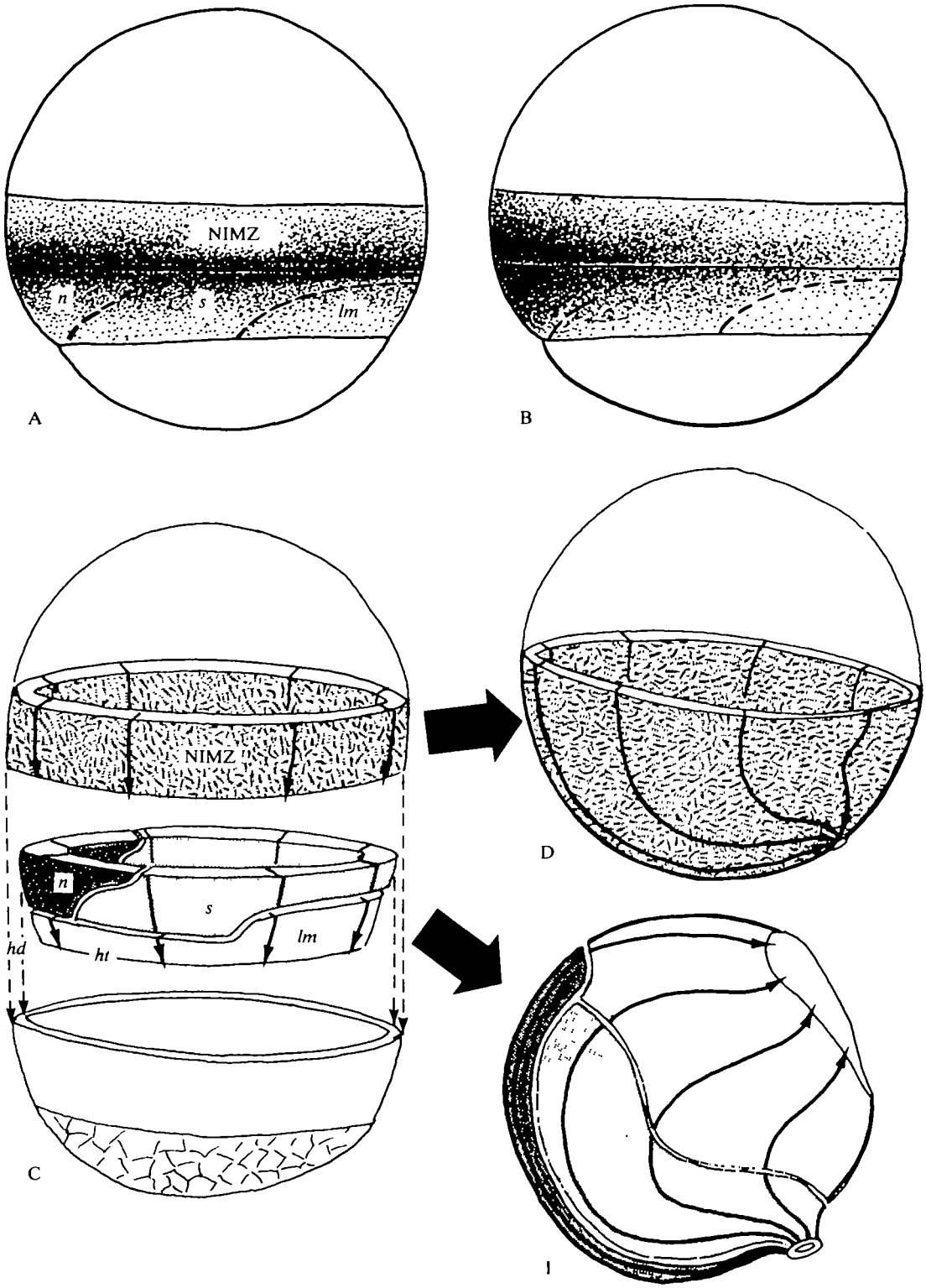

Fig. 12. The prospective movements of convergence (A) and extension (B) of the IMZ and NIMZ of the *Xenopus* early gastrula are represented diagramatically by shading, the denser the shading the greater degree. The prospective areas of the notochord (*n*), somitic mesoderm (*s*), and lateral and ventral mesoderm (*lm*) in the deep IMZ are indicated. In an exploded diagram of the early gastrula, the NIMZ and deep IMZ are shown with meridian lines (C). The tissue deformations bought about by exercise of convergence and extension in these regions during gastrulation is shown for the NIMZ (D) and the deep IMZ (mesodermal mantle) (E) in corresponding diagrams of the late gastrula. For completeness, the anterior, dorsal mesoderm (prospective head (*hd*) and heart (*ht*) mesoderm) is included (C) even though it has involuted by the early gastrula stage (Keller, 1976).

explants or in exogastrulae. Thus the highly patterned, active convergent extension of the dorsal NIMZ in explants undoubtedly occurs *in vivo* as well. Moreover, these powerful movements, which mimic the movements of the neural ectoderm (see Jacobson & Gordon, 1976), are unmistakably well under way very early, by stage 11, some time before the earliest appearance of molecular markers characteristic of neural tissue (see Kintner & Melton, 1987; Sharpe *et al.* 1987).

However, the dorsal NIMZ extends only if it has basal contact with itself in sandwich explants or with involuted chordamesoderm (dorsal IMZ) *in vivo*, but not in open-faced explants where its basal surface is exposed (Keller *et al.* 1985*a*,*b*). This requirement for basal contact may ensure that the dorsal NIMZ will exercise convergent extension only when the IMZ underlies it in normal development (see Keller *et al.* 1985*b*). Jacobson (1981, 1985) has shown that the corresponding region of the newt, the 'notoplate', must have basal contact with the underlying notochord in order to function in elongation of the neural plate. Not only does the NIMZ require basal contact, it thins more and extends faster than the IMZ.Thus, the *Xenopus* embryo may have two region-specific cellular mechanisms of convergent extension, one in the IMZ and one in the NIMZ.

Convergence and extension in abnormal gastrulation

Because dorsal, axial tissues extend more than ventral ones, the blastopore closes asymmetrically over the ventral side of the yolky endoderm. Therefore, ventralized embryos, produced by u.v. irradiation in the first cell cycle, and lacking dorsal, axial structures (Scharf & Gerhart, 1980) should close their blastopores by convergence with no more extension than is normally seen on the ventral side. Thus, their blastoporal lips should collapse inward, with a corresponding reduction in the circumference of the embryonic profile. Conversely, 'hyperdorsal' embryos produced by exposure to heavy water (Gerhart *et al.* 1983) or lithium (Kao *et al.* 1986), must show the powerful dorsal-type extension in all sectors. Since there is no weakly-extending ventral sector to accommodate such extension in hyperdorsal embryos, their blastoporal lips meet and then extension continues to form proboscis-like structures often seen in these embryos.

Function of convergent extension in gastrulation of other amphibians

Autonomous convergence and extension play a large role in gastrulation of two anurans, *Hyla regilla* (Schechtman, 1942) and *Xenopus*. In contrast, the failure of sandwich explants of the DMZ of the urodele *Pleurodeles waltlii* to extend until late gastrulation suggests that urodele gastrulation may depend more on mesodermal cell migration and less on convergence and extension (Shi *et al.* 1987). Explants of the DMZ of the urodele, *Ambystoma mexicanum* (the Mexican axolotl) also converge and extend little until the late gastrula stage (Keller, unpublished results). But these negative results may be due to inappropriate conditions. It is perhaps relevant that extension of the notoplate region of the urodele neurula depends on its boundaries with other tissues (Jacobson, 1981). On the other hand, these observations may reflect a real difference between species. Convergence and extension movements may be important for neurulation in all anurans and urodeles but also occur during gastrulation of *Xenopus* and *Hyla*, where they help to enclose the relatively large yolk plug. Early onset of these movements may also increase the rate of gastrulation in these relatively fast-developing embryos. However, it is premature to conclude that differences in fate maps and gastrulation movements among the few species of urodeles and anurans examined thus far are characteristic of their respective orders (see Keller, 1986). More species of anurans and urodeles, not to mention caecilians, should be examined to determine which features of gastrulation are common to all three orders and which features, if any, are unique to each order.

We are grateful to Paul Tibbetts for his excellent technical assistance, to Paul Wilson, Jeff Hardin and Ann Sutherland for their comments and suggestions, and to Jiro Okochi for his reliable care of our frogs. This work was supported by NIH grant HD189790 to Ray Keller and NIH Postdoctoral fellowship grant GM08738 to Mike Danilchik.

References

Akers, R. M., Phillips, C. R. & Wessells, N. K. (1986). Expression of an epidermal antigen used to study tissue induction in the early *Xenopus laevis* embryo. *Science* **231**, 613–616.

Bijtel, J. H. (1958). The mode of growth of the tail in urodele larvae. *J. Embryol. exp. Morph.* **6**, 466–478.

Cooke, J. & Smith, J. C. (1987). The midblastula cell cycle transition and the character of mesoderm in U.V.-induced nonaxial *Xenopus* development. *Development* **90**, 197–210.

Cooke, J. & Weber, J. A. (1985*a*). Dynamics of the control of body pattern formation in *Xenopus laevis*. I. Timing and pattern in the development of dorso-anterior and of posterior blastomere pairs isolated at the 4 cell stage. *J. Embryol. exp. Morph.* **88**, 85–112.

Cooke, J. & Weber, J. A. (1985*b*). Dynamics of the control of body pattern formation in *Xenopus laevis*. II. Timing and pattern in the development of single blastomeres (presumptive lateral halves) isolated at the 2-cell stage. *J. Embryol. exp. Morph.* **88**, 113–133.

DALE, L. & SLACK, J. M. W. (1987). Regional specification within the mesoderm of early embryos of *Xenopus laevis*. *Development* **100**, 279–295.

GERHART, J., BLACK, S., GIMLICH, R. & SCHARF, S. (1983). Control of polarity in the amphibian egg. In *Time, Space and Pattern in Embryonic Development*, pp. 261–286. New York: Alan Liss, Inc.

GERHART, J. & KELLER, R. (1986). Region-specific Cell Activities in Amphibian Gastrulation. *A. Rev. Cell Biol.* **2**, 201–229.

HARDIN, J. & KELLER, R. (1988). The role of bottle cells in gastrulation of *Xenopus laevis*. *Development* **103**, 211–230.

HOLTFRETER, J. (1933). Die totale Exogastrulation, eine Selbstablosung des Ektoderms von Entomesoderm. *Arch. Entwmech.* **129**, 669–793.

HOLTFRETER, J. (1938*a*). Differenzierungspotenzen isolieter Teile der Urodelengastrula. *Wilhelm Roux' Arch. EntwMech. Org.* **138**, 522–656.

HOLTFRETER, J. (1938*b*). Differenzierungspotenzen isolieter Teile der Anurengastrula. *Wilhelm Roux' Arch. EntwMech. Org.* **138**, 657–738.

HOLTFRETER, J. (1943*a*). Properties and function of the surface coat in amphibian embryos. *J. exp. Zool.* **93**, 251–323.

HOLTFRETER, J. (1943*b*). A study of the mechanics of gastrulation. Part I. *J. exp. Zool.* **94**, 261–318.

HOLTFRETER, J. (1944). A study of the mechanics of gastrulation. Part II. *J. exp. Zool.* **95**, 171–212.

IKUSHIMA, N. & MARUYAMA, S. (1971). Structure and developmental tendency of the dorsal marginal zone in the early amphibian gastrula. *J. Embryol. exp. Morph.* **25**, 263–276.

JACOBSON, A. (1981). Morphogenesis of the neural plate and tube. In *Morphogenesis and Pattern Formation* (ed. T. G. Connelly, L. Brinkley & B. Carlson), pp. 223–263. New York: Raven Press.

JACOBSON, A. (1985). Adhesion and movement of cells may be coupled to produce neurulation. In *The Cell in Contact: Adhesions and Junctions as Morphogenetic Determinants* (ed. G. M. Edelman & J.-P. Thiery), pp. 49–65. New York: John Wiley & Sons.

JACOBSON, A. & GORDON, R. (1976). Changes in the shape of the developing vertebrate nervous system analyzed experimentally, mathematically, and by computer simulation. *J. exp. Zool.* **197**, 191–246.

KAO, K. R., MASUI, Y. & ELINSON, R. (1986). Lithium-induced respecification of pattern in *Xenopus laevis* embryos. *Nature, Lond.* **322**, 371–373.

KELLER, R. E. (1975). Vital dye mapping of the gastrula and neurula of *Xenopus laevis*. I. Prospective areas and morphogenetic movements of the superficial layer. *Devl Biol.* **42**, 222–241.

KELLER, R. E. (1976). Vital dye mapping of the gastrula and neurula of *Xenopus laevis*. II. Prospective areas and morphogenetic movements in the deep region. *Devl Biol.* **51**, 118–137.

KELLER, R. E. (1978). Time-lapse cinemicrographic analysis of superficial cell behavior during and prior to gastrulation in *Xenopus laevis*. *J. Morph.* **157**, 223–248.

KELLER, R. E. (1980). The cellular basis of epiboly: An SEM study of deep-cell rearrangement during gastrulation in *Xenopus laevis*. *J. Embryol. exp. Morph.* **60**, 201–234.

KELLER, R. E. (1981). An experimental analysis of the role of bottle cells and the deep marginal zone in gastrulation of *Xenopus laevis*. *J. exp. Zool.* **216**, 81–101.

KELLER, R. E. (1984). The cellular basis of gastrulation in *Xenopus laevis*: active, postinvolution convergence and extension by mediolateral interdigitation. *Am. Zool.* **24**, 589–603.

KELLER, R. E. (1986). The cellular basis of amphibian gastrulation. In *Developmental Biology: A Comprehensive Synthesis*. Vol. 2. *The Cellular Basis of Morphogenesis* (ed. L. Browder), pp. 241–327. New York: Plenum Press.

KELLER, R. E., DANILCHIK, M., GIMLICH, R. & SHIH, J. (1985*a*). Convergent extension by cell intercalation during gastrulation of *Xenopus laevis*. In *Molecular Determinants of Animal Form* (ed. G. M. Edelman). *UCLA Symp. Mol. Cell. Biol.*, vol. 31, pp. 111–141. New York: Alan R. Liss, Inc.

KELLER, R. E., DANILCHIK, M., GIMLICH, R. & SHIH, J. (1985*b*). The function and mechanism of convergent extension during gastrulation of *Xenopus laevis*. *J. Embryol. exp. Morph.* **89, Supplement**, 185–209.

KELLER, R. E. & HARDIN, J. D. (1987). Cell behavior during active cell rearrangement: evidence and speculations. *J. Cell Sci.* (in press).

KELLER, R. E. & SCHOENWOLF, G. C. (1977). An SEM study of cellular morphology, contact, and arrangement, as related to gastrulation in *Xenopus laevis*. *Wilhelm Roux' Arch. devl Biol.* **182**, 165–186.

KINTNER, C. R. & MELTON, D. A. (1987). Expression of Xenopus N-CAM RNA in ectoderm is an early response to neural induction. *Development* **99**, 311–325.

KUBOTA, H. & DURSTON, A. J. (1978). Cinematographical study of cell migration in the opened gastrula of *Ambystoma mexicanum*. *J. Embryol. exp. Morph.* **44**, 71–80.

NAKATSUJI, N. (1974). Studies on the gastrulation of amphibian embryos; pseudopodia in the gastrula of *Bufo bufo japonicus* and their significance to gastrulation. *J. Embryol. exp. Morph.* **32**, 795–804.

NAKATSUJI, N. (1975). Studies on the gastrulation of amphibian embryos: Cell movement during gastrulation in *Xenopus laevis* embryos. *Wilhelm Roux' Arch. devl Biol.* **178**, 1–14.

NAKATSUJI, N., GOULD, A. C. & JOHNSON, K. (1982). Movement and guidance of migrating mesodermal cells in *Ambystoma maculatum* gastrulae. *J. Cell Sci.* **56**, 207–222.

NIEUWKOOP, P. & FABER, J. (1967). *Normal Table of* Xenopus laevis (*Daudin*). Second edition. Amsterdam: North-Holland Publishing Company.

SCHARF, S. R. & GERHART, J. C. (1980). Determination of the dorsal-ventral axis in eggs of *Xenopus laevis*: Complete rescue of UV-impaired eggs by oblique

orientation before first cleavage. *Devl Biol* **79**, 181–198.

SCHECHTMAN, A. M. (1942). The mechanism of amphibian gastrulation. I. Gastrulation-promoting interactions between various regions of an anuran egg (*Hyla regilla*). *Univ. Calif. Publ. Zool.* **51**, 1–39.

SHARPE, C. R., FRITZ, A., DE ROBERTIS, E. M. & GURDON, J. B. (1987). A homeobox-containing marker of posterior neural differentiation shows the importance of predetermination in neural induction. *Cell* **50**, 749–758.

SHI, D.-L., DELARUE, M., DARRIBERE, T., RIOU, J.-F. & BOUCAUT, J.-C. (1987). Experimental analysis of the extension of the dorsal marginal zone in *Pleurodeles walti* gastrulae. *Development* **100**, 147–161.

SLACK, J. M. W. (1985). Peanut lectin receptors in the early amphibian embryo: regional markers for the study of embryonic induction. *Cell* **41**, 237–247.

SLACK, J. M. W. & FORMAN, D. (1980). An interaction between dorsal and ventral regions of the marginal zone in early amphibian embryos. *J. Embryol. exp. Morph.* **56**, 283–299.

SPEMANN, H. (1938). *Embryonic Development and Induction*. New York: Yale University Press. Reprinted 1962. Hafner Publishing Company, Inc.

VOGT, W. (1922). Die Einrollung und Streckung der Urmundlippen bei Triton nach Versuchen mit einer neuen Methode embryonaler transplantation. *Verh. Zool. Ges.* **27**, 49–51.

VOGT, W. (1929). Gestaltungsanalyse am Amphibienkeim mit ortlicher Vitalfarbung. II. Teil. Gastrulation und Mesodermbildung bei Urodelen und Anuren. *Wilhelm Roux Arch. EntwMech. Org.* **120**, 384–706.

YOUN, B.-W., KELLER, R. E. & MALACINSKI, G. M. (1981). An atlas of notochord and somite morphogenesis in several Anuran and Urodelean Amphibians. *J. Embryol. exp. Morph.* **59**, 365–384.

(*Accepted 26 January 1988*)